JOURNAL OF Materials CHEMISTRY

Structure and thermoelectric properties of the new quaternary tin selenide $K_{1-x}Sn_{5-x}Bi_{11+x}Se_{22}$

Antje Mrotzek,[a] Duck-Young Chung,[a] Tim Hogan[b] and Mercouri G. Kanatzidis*[a]

[a]*Department of Chemistry and Center for Fundamental Materials Research, Michigan State University, East Lansing, MI 48834, USA*
[b]*Department of Electrical and Computer Engineering, Michigan State University, East Lansing, MI 48834, USA*

Received 5th January 2000, Accepted 15th March 2000
Published on the Web 9th June 2000

Silver colored ribbon-like crystals of $K_{1-x}Sn_{5-x}Bi_{11+x}Se_{22}$ ($x \approx 0.33$) were prepared by direct combination of K_2Se, Bi_2Se_3, Sn and Se at 800 °C. A structure determination was carried out for $K_{0.66}Sn_{4.82}Bi_{11.18}Se_{22}$. Bi_2Te_3-type and NaCl-type building units are connected to form a new kind of three-dimensional anionic framework with K^+ filled tunnels. The building units are assembled from distorted, edge-sharing (Bi,Sn)Se_6 octahedra. Bi and Sn atoms are disordered over all metal sites of the chalcogenide network while the K site is only one third occupied. The charge transport measurements of $K_{0.66}Sn_{4.82}Bi_{11.18}Se_{22}$ at room temperature reveal an electrical conductivity of 450 S cm^{-1} and a thermopower of -43 μV K^{-1}. The thermal conductivity is 1.5 W m^{-1} K^{-1}. An optical band gap of approximately 0.12 eV was determined at room temperature. $K_{0.66}Sn_{4.82}Bi_{11.18}Se_{22}$ melts congruently at 680 °C.

Introduction

Currently there is great interest in finding new materials[1] with superior thermoelectric properties[2] and in developing new concepts for designing new thermoelectric compounds.[3] The thermoelectric properties are characterized by the figure of merit $Z \cdot T$ with the absolute temperature T and $Z = \sigma \cdot S^2/\kappa$ where σ is the electrical conductivity, S is the thermopower and κ is the total thermal conductivity. The best known thermoelectric materials are various alloys of Bi_2Te_3; they exhibit a figure of merit about 1.[4] Because no theoretical limit[5] has been found for the figure of merit the motivation for exploring new materials is strong. Our research is focussed on obtaining heavy element chalcogenide compounds with high electrical conductivity σ, high Seebeck coefficient S and low thermal conductivity κ for $Z \cdot T$ maximization. The complex chalcogenides $BaBiTe_3$,[6] $K_2Bi_8Se_{13}$,[7,8] $K_{2.5}Bi_{8.5}Se_{14}$,[8,9] $CsBi_4Te_6$[8,10] and $KBi_{6.33}S_{10}$[7] exhibit promising thermoelectric properties. In these examples, the alkali and alkaline earth metals are incorporated in structurally diverse bismuth chalcogenide frameworks. The electropositive metal ions stabilize the anionic frameworks by ionic bonding and they tend to fill tunnels in the structure where they can function as "rattlers" to reduce the lattice thermal conductivity.[3,8] According to the Mott formula,

$$S = \frac{\pi^2}{3} \cdot \frac{k^2 T}{e} \cdot \frac{\mathrm{d} \ln \sigma(E)}{\mathrm{d}E}\bigg|_{E=E_f}$$

with k = Boltzmann constant, T = absolute temperature, e = elementary charge, $\sigma(E)$ = electrical conductivity at energy E, E_f = Fermi energy, the electrical conductivity σ and the thermopower S are related to the electronic band structure. If doped appropriately, a more complex crystal structure and composition may generate a more complex electrical band structure that may give rise to more favorable thermoelectric properties. Therefore the investigations were extended to quaternary systems. The attempt to incorporate Pb metal in the K/Bi/Se or K/Sb/Se system led to the compounds $A_{1+x}Pb_{4-2x}M_{7+x}Se_{15}$ with A = K, Rb and M = Bi, Sb[11] with interesting electrical properties. In these compounds the alkali metal, lead and bismuth (or antimony) atoms are found to occupy the same crystallographic sites, probably due to the size similarities of these species. Because of the isovalent relationship between Pb and Sn we are interested in analogous compounds in the system K/Sn/Bi/Se as well. A probable disorder of Sn with Bi or alkali metal, similar to the one found in the Pb compounds, would introduce randomness of the mass, size and charge of the atoms on a particular lattice position and decrease the thermal conductivity. We report here the syntheses, structural and physicochemical characterization of the new quaternary compound $K_{0.66}Sn_{4.82}Bi_{11.18}Se_{22}$, which reveals a new structure-type.

Experimental

Reagents

Chemicals in this work were used as obtained: (i) tin metal, 99.999%, 200 mesh, Cerac, Milwaukee, WI; (ii) bismuth chunks, 99.999%, Noranda Advanced Materials, Quebec, Canada; (iii) selenium shots, 99.999%, Noranda Advanced Materials, Quebec, Canada; (iv) potassium metal, analytical reagent, Mallinckrodt Inc., Paris, KY.

Synthesis

All manipulations were carried out under a dry nitrogen atmosphere in a Vacuum Atmospheres Dri-Lab glovebox. Bi_2Se_3 was obtained by reaction of stoichiometric amounts of the elements in evacuated silica glass ampoules at 800 °C for 3 days. K_2Se was prepared by stoichiometric reaction of potassium and selenium in liquid ammonia.

$K_{0.66}Sn_{4.82}Bi_{11.18}Se_{22}$. Method I. A mixture of K_2Se (0.5 mmol), tin metal (3 mmol), selenium (2 mmol) and Bi_2Se_3 (6.5 mmol) was loaded in a carbon-coated silica tube (9 mm diameter) and sealed at a residual pressure of $< 10^{-4}$ Torr. The starting materials were heated within 24 hours to 800 °C and kept there for 24 hours, followed by

DOI: 10.1039/b000045k

slow cooling to 400 °C at a rate of −0.1 °C min^{-1} and to 50 °C in 10 hours. A silver shiny ingot of pure $K_{0.66}Sn_{4.82}Bi_{11.18}Se_{22}$ was obtained after washing any impurities with dimethylformamide (DMF), methanol and diethyl ether.

$K_{0.66}Sn_{4.82}Bi_{11.18}Se_{22}$. Method II. Needle-like, single crystals of $K_{0.66}Sn_{4.82}Bi_{11.18}Se_{22}$ were obtained in a mixture with composition "$KSn_4Bi_7Se_{15}$" by reaction of the starting materials in the ratio $K_2Se : Sn : Bi_2Se_3 : Se = 1 : 4 : 4 : 4$. The starting materials were heated within 24 hours to 800 °C and kept there for 72 hours, followed by slowly cooling to 400 °C at a rate of −5 °C h^{-1}, then to 100 °C at a rate of −15 °C h^{-1} and to 50 °C in 1 hour. Microprobe analysis with a SEM/EDS system performed on eight different crystals gave an average composition of $K_{0.8}Sn_{3.9}Bi_{11.4}Se_{22}$.

Physical measurements

Electron microscopy. Quantitative microprobe analyses of the compound were performed with a JEOL JSM-35C SEM equipped with a Tracer Northern EDS detector. Data were acquired using an accelerating voltage of 25 kV and a 60 s accumulation time.

Differential thermal analysis. Differential thermal analysis (DTA) was performed with a computer-controlled Shimadzu DTA-50 thermal analyzer. A sample of ground crystalline material (~20 mg total mass) was sealed in a carbon-coated silica ampoule under vacuum. A silica ampoule containing alumina of equal mass was sealed under vacuum and placed on the reference side of the detector. The sample was heated to 900 °C at 10 °C min^{-1}, then isothermed for 5 min, followed by cooling at 10 °C min^{-1} to 150 °C and finally by rapid cooling to room temperature. The stability/reproducibility of the sample was monitored by running multiple heating/cooling cycles. The DTA sample was examined by powder X-ray diffraction after the experiment.

Infrared spectroscopy. Diffuse reflectance measurements were made on the finely ground sample at room temperature. The spectrum was recorded in the infrared region (6000–400 cm^{-1}) with the use of a Nicolet MAGNA-IR 750 spectrometer equipped with a collector diffuse reflectance accessory from Spectra-Tech. Inc. Absorption (α/S) data were calculated from the reflectance data using the Kubelka–Munk function:[12] $\sigma/S = (1-R)^2/2R$, where R is the reflectance at a given energy, α is the absorption coefficient and S is the scattering coefficient. The scattering coefficient is practically energy independent for particles larger than 5 μm, which is smaller than the particle size of the sample used here. The band gap was determined as the intersection point between the energy axis at the absorption offset and the line extrapolated from the linear portion of the absorption edge in a α/S *vs.* E (eV) plot.

Charge transport measurements. Direct current (dc) electrical conductivity and thermopower measurements were made on an ingot and a pressed pellet, respectively. Room temperature conductivity measurements were performed in the usual four-probe geometry. The Seebeck coefficient was measured between 80 and 400 K for obtaining low temperature data and between 300 and 600 K for high temperature measurements by using a SB-100 Seebeck Effect Measurement System, MMR Technologies, Inc.

A four-sample measurement system was used to measure thermal conductivity.[13] To fully characterize the figure of merit, the properties were measured for each sample over the selective temperature range of interest of 77 K to 320 K (system capability is 4.2 K to 475 K). To alleviate offset error voltages and increase the density of data points, a slow ac technique was used with a heater pulse period of 720 s.[14] The pulse shape is monitored, *in situ*, to determine temperature stabilization, and the sample chamber was maintained at a pressure less than 10^{-5} Torr for the entire measurement run. Samples were mounted in the standard four probe configuration for the thermal conductivity, and the heater current was adjusted for an average temperature gradient of 1 K. The sample stage and radiation shield are gold coated copper to minimize radiation effects and maintain temperature uniformity. All electrical leads were 25 μm in diameter with lengths greater than 10 cm to minimize thermal conduction losses. Data acquisition and computer control of the system was maintained under the LabVIEW[15] software environment.

Powder X-ray diffraction. Powder patterns of all starting materials and products were obtained using a Rigaku-Denki/Rw400F2 (rotaflex) rotating-anode powder diffractometer and a CPS 120 INEL X-ray powder diffractometer equipped with a position-sensitive detector. The purity and homogeneity were confirmed by comparing the X-ray powder diffraction pattern to that calculated from single crystal data using the CERIUS^2 software.[16]

Single crystal X-ray crystallography. A single crystal ($0.04 \times 0.04 \times 1.38$ mm) was mounted on the tip of a glass fiber. The intensity data were collected on a Siemens SMART Platform CCD diffractometer using graphite monochromatized Mo Kα radiation. The SMART software[17] was used for data acquisition. The extraction and reduction of the data were performed with the program SAINT.[18] The observed systematic absences led to the space group $P2_1/m$. A semi-empirical absorption correction based on symmetrically equivalent reflections was done using the program SADABS.[19] The crystal structure was solved with direct methods (SHELXS-97[20]). All structure refinements were performed using the SHELXTL package of crystallographic programs.[20]

Twenty crystallographically independent positions (Bi1–7, Sn1, Se1–11 and K1) were found situated on mirror planes ($y = 1/4$ and 3/4). This leads to the ideal formula $KSn_5Bi_{11}Se_{22}$ which is charge balanced assuming K^{1+}, Sn^{2+}, Bi^{3+} and Se^{2-}. The elemental composition (determined by EDS), charge balance requirements and anomalous thermal atomic displacement parameters (ADPs) for all metal sites indicated disorder at the metal sites. Therefore, all bismuth and tin sites were refined with mixed Bi/Sn occupancy with the sum of occupancies constrained to be equal to 0.5 (fully occupied). The refinement resulted in 21% Sn in the Bi1 and the Bi2 sites, respectively, 28% Sn in the Bi3 site, 10% Sn in the Bi4 site, 33% Sn in the Bi5 site, 28% Sn in the Bi6 site, 11% Sn in the Bi7 site and 11% Bi in the Sn1 site. The remaining ADPs of the potassium sites of 15.54 Å^2 also introduced a disorder model at the K site. The refinement converged at partial K atom occupancy of 0.17(1) equal to 1/3 occupied. The final formula $K_{0.66(4)}Sn_{4.82(7)}Bi_{11.18(7)}Se_{22}$ is charge balanced within standard deviation. After anisotropic refinement the $R1$ and $wR2$ values dropped from 7.3% and 13.0% to 5.4% and 9.3% respectively. The results of the structure refinement and other crystallographic data are given in Tables 1, 2 and 3.

CCDC reference number 1145/216.

Results and discussion

Structure description

$K_{0.66}Sn_{4.82}Bi_{11.18}Se_{22}$ adopts the monoclinic space group $P2_1/m$ with one formula per unit cell. The structure is composed of twenty crystallographically inequivalent atoms: Bi1 through Bi7, Sn1, K1 and Se1 through Se11 are all located on mirror planes perpendicular to the short b-axis. Fig. 1 and 2 show projections of the structure on the ac-plane. The basic building

Table 1 Summary of crystallographic data and structural analysis

Formula	$K_{0.66(4)}Sn_{4.82(7)}Bi_{11.18(7)}Se_{22}$
Formula weight	4939.32
Crystal system	monoclinic
Space group	$P2_1/m$
a/Å	15.777(2)
b/Å	4.1669(6)
c/Å	17.358(2)
β/°	99.249(2)
Z; V/Å^3	1, 1126.24
T/K	293
μ(Mo Kα)/cm^{-1}	73.42
Total data measured	10967
Total unique data	3003
Data with $I>2\sigma(I)$	2478
No. of variables	150
Final $R1/wR2^a$ (%)	5.35/9.32

$^aR1=\Sigma||F_o|-|F_c||/\Sigma|F_o|$, $wR2=\{\Sigma[w(F_o^2-F_c^2)^2]/\Sigma[w(F_o^2)^2]\}^{1/2}$.

Table 2 Fractional atomic coordinates ($y=0.25$) and equivalent atomic displacement parameters (U_{eq}) values in 10^{-3} Å^2 for $K_{0.66}Sn_{4.82}Bi_{11.18}Se_{22}$ with estimated standard deviations in parentheses

	x	z	sof	$U_{eq}{}^a$
Bi1/Sn1′	0.27946(6)	0.04699(5)	0.79(1)/0.21	21.6(3)
Bi2/Sn2′	0.66938(5)	0.74323(5)	0.794(9)/0.206	18.5(3)
Bi3/Sn3′	0.37311(6)	0.46652(5)	0.716(9)/0.284	20.0(3)
Bi4/Sn4′	0.58414(5)	0.31820(4)	0.90(1)/0.10	20.5(3)
Bi5/Sn5′	0.46499(6)	0.89101(5)	0.67(1)/0.33	19.3(4)
Bi6/Sn6′	0.94418(6)	0.70750(5)	0.72(1)/0.28	25.0(3)
Bi7/Sn7′	0.90311(5)	0.43776(5)	0.89(1)/0.11	20.1(3)
Sn1/Bi1′	0.8278(1)	0.17596(8)	0.89(1)/0.11	34.5(6)
K1	0.988(1)	0.992(1)	0.33(2)	110(12)
Se1	0.8000(1)	0.8774(1)	1	18.7(4)
Se2	0.2450(1)	0.3265(1)	1	18.1(4)
Se3	0.7102(1)	0.4602(1)	1	19.4(4)
Se4	0.3337(1)	0.7574(1)	1	19.5(4)
Se5	0.6215(1)	0.0356(1)	1	22.2(5)
Se6	0.4378(1)	0.1839(1)	1	15.6(4)
Se7	0.5195(1)	0.6053(1)	1	16.1(4)
Se8	0.0088(1)	0.1870(1)	1	20.5(5)
Se9	0.0784(1)	0.4388(1)	1	15.8(4)
Se10	0.1111(1)	0.6831(1)	1	18.4(4)
Se11	0.1463(2)	0.9271(1)	1	32.5(6)

$^aU_{eq}$ is defined as one-third of the trace of the orthogonalized U_{ij} tensor.

blocks, which comprise the entire framework, are fragments "cut out" of the Bi_2Te_3 and the NaCl lattices.

Step shaped layers of Bi_2Te_3-type units are connected *via* NaCl-type units to a three-dimensional anionic framework with potassium-filled tunnels running along the *b*-axis. Ribbon-like fragments excised from a Bi_2Te_3 layer that are five Bi octahedra wide are re-connected in a *trans–trans* fashion to build the step shaped layers which extend over the *bc*-plane. The Bi_2Te_3-type units are built by edge sharing of distorted (Bi,Sn)Se_6 octahedra. The local Bi(Sn) distortion to a 3+3 coordination is due to the lone pairs of Bi^{3+} and Sn^{2+} respectively. The same layers of Bi_2Te_3 units are found in the structure of $K_{1+x}Pb_{4-2x}Bi_{7+x}Se_{15}$ with $x=0.25$[11] ($a=17.4481(8)$ Å, $b=4.1964(2)$ Å, $c=21.6945(10)$ Å, $\beta=98.850(1)^\circ$) (compare Fig. 2). The mean Bi(Sn)–Se distance of 2.97 Å in the Bi_2Te_3-type layers of $K_{0.66}Sn_{4.82}Bi_{11.18}Se_{22}$ is comparable to the corresponding value (2.99 Å) for $K_{1+x}Pb_{4-2x}Bi_{7+x}Se_{15}$ ($x=0.25$). There is no obvious relation between the extent of the distortion from an ideal octahedral coordination to three shorter and three longer distances and the contribution of Sn on the crystallographically distinguished sites. Sn seems to be randomly distributed over all Bi sites, with content ranging from 10% Sn on the Bi4 site up to 33% Sn for the Bi5 site.

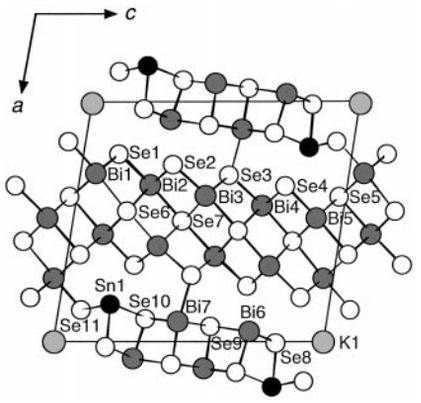

Fig. 1 The structure of $K_{0.66}Sn_{4.82}Bi_{11.18}Se_{22}$ with atom labeling.

It is obvious from Fig. 2 that the NaCl-type blocks in $K_{0.66}Sn_{4.82}Bi_{11.18}Se_{22}$ are only half as thick as those in $K_{1+x}Pb_{4-2x}Bi_{7+x}Se_{15}$ ($x=0.25$). The NaCl-type units in both compounds are three Bi octahedra wide in the direction parallel to the Bi_2Te_3-type layers. In the direction perpendicular to the Bi_2Te_3-type layers the NaCl-type block is one Bi

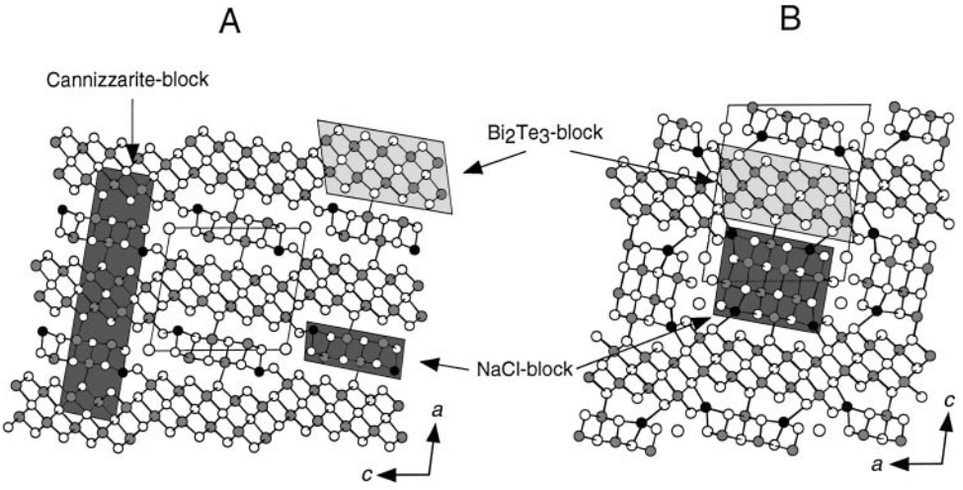

Fig. 2 (A) A larger section of the structure of $K_{0.66}Sn_{4.82}Bi_{11.18}Se_{22}$ viewed down the *b*-axis. The cannizzarite-like block is shown as a shaded area. (B) The structure of $K_{1.25}Pb_{2.5}Bi_{7.25}Se_{15}$ viewed down the *b*-axis. Small white spheres: Se, large light-gray spheres: K, middle-gray spheres: Bi, dark-gray spheres: Sn and Pb respectively. The archetypal Bi_2Te_3- and NaCl-type building units are highlighted in both structures.

Table 3 Selected distances in Å for $K_{0.66}Sn_{4.82}Bi_{11.18}Se_{22}$. Because of the mixed Bi/Sn occupancy on all metal sites, these distances represent only average values

Bi1	–Se11	2.720(2)	Bi2	–Se1	2.851(2)
	–Se1 × 2	2.857(1)		–Se2 × 2	2.855(1)
	–Se5 × 2	3.092(2)		–Se6 × 2	3.080(1)
	–Se6	3.159(2)		–Se 7	3.083(2)
Bi3	–Se3 × 2	2.868(1)	Bi4	–Se4 × 2	2.879(1)
	–Se2	2.901(2)		–Se3	2.908(2)
	–Se7	3.057(2)		–Se6	3.006(2)
	–Se7 × 2	3.073(1)		–Se7 × 2	3.079(1)
Bi5	–Se4	2.850(2)	Bi6	–Se10	2.733(2)
	–Se5 × 2	2.895(1)		–Se8 × 2	2.794(1)
	–Se6 × 2	3.004(1)		–Se9 × 2	3.260(2)
	–Se5	3.225(2)		–Se2 × 2	3.610(2)
Bi7	–Se9	2.763(2)	Sn1	–Se11 × 2	2.807(2)
	–Se10 × 2	2.939(1)		–Se8	2.830(3)
	–Se9 × 2	2.969(1)		–Se10 × 2	3.240(2)
	–Se3	3.129(2)		–Se4 × 2	3.622(2)
				–Se5	3.739(3)
K1	–K1 × 2	2.127(9)			
	–Se11	2.91(2)			
	–Se1	3.30(2)			
	–Se8	3.35(2)			
	–Se11 × 2	3.44(2)			
	–Se8 × 2	3.75(2)			
Se1	–Bi2	2.851(2)	Se2	–Bi2 × 2	2.855(1)
	–Bi1 × 2	2.857(1)		–Bi3	2.901(2)
	–K1	3.30(2)		–Se9	3.516(3)
	–Se11 × 2	3.970(2)		–Bi6 × 2	3.610(2)
	–Se8 × 2	3.972(2)			
Se3	–Bi3 × 2	2.868(1)	Se4	–Bi5	2.850(2)
	–Bi4	2.908(2)		–Bi4 × 2	2.879(1)
	–Bi7	3.129(2)		–Se10	3.542(3)
				–Sn1 × 2	3.622(2)
Se5	–Bi5 × 2	2.895(1)	Se6	–Bi5 × 2	3.004(1)
	–Sn1 × 2	3.092(2)		–Bi4	3.006(1)
	–Bi5	3.225(2)		–Bi2 × 2	3.080(1)
	–Sn1	3.739(3)		–Bi1	3.159(2)
Se7	–Bi3	3.057(2)		–Bi6 × 2	2.794(1)
	–Bi3 × 2	3.073(1)		–Sn1	2.830(3)
	–Bi4 × 2	3.079(1)		–K1	3.349(3)
	–Bi2	3.083(2)		–Se11 × 2	3.555(2)
				–K1 × 2	3.748(9)
				–Se10 × 2	3.790(2)
				–Se1 × 2	3.972(2)
Se9	–Bi7	2.763(2)	Se10	–Bi6	2.733(2)
	–Bi7 × 2	2.969(1)		–Bi7 × 2	2.939(1)
	–Bi6 × 2	3.260(2)		–Sn1 × 2	3.240(2)
	–Se2	3.516(3)		–Se4	3.542(3)
	–Se10 × 2	3.965(2)		–Se8 × 2	3.790(2)
				–Se9 × 2	3.965(2)
Se11	–Bi1	2.720(2)			
	–Sn1 × 2	2.807(2)			
	–K1	2.91(2)			
	–K2 × 2	3.44(2)			
	–Se8 × 2	3.555(2)			
	–Se1 × 2	3.970(2)			

octahedron high in the tin compound and two Bi octahedra high in the lead compound. Atom Bi7 connects the NaCl-type unit with the Bi_2Te_3-type unit by a relatively strong interaction with Se3 ($d_{Bi7–Se3} = 3.13$ Å). This prominent crystallographic position contains 11% Sn atoms. The five-coordinated Bi6 and Sn1 sites contain 28% Sn and 11% Bi respectively. In this part of the structure Sn seems to prefer a five-coordinated environment. The Se atoms 4 ($d_{Sn1–Se4} = 3.62$ Å × 2) and 5 ($d_{Sn1–Se5} = 3.74$ Å) of the Bi_2Te_3-type units complete the coordination of Sn1 to a distorted bi-capped trigonal prism. For Bi6 the far distant Se2 ($d_{Bi6–Se2} = 3.61$ Å × 2) extends the coordination polyhedron from a tetragonal pyramid to an extremely distorted capped octahedron (see Fig. 3).

The potassium ions fill the tunnels created by the linkage of the two different structure units. The tri-capped trigonal prismatic sites are only 33% occupied. The high ADP of this site suggests that the potassium ions "rattle" in their positions although, probably, static disorder along the tunnel direction is also present.

The structure of $K_{0.66}Sn_{4.82}Bi_{11.18}Se_{22}$ has elements of the

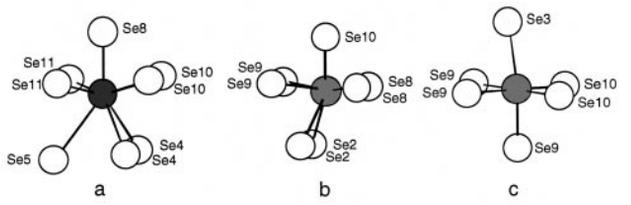

Fig. 3 Local coordination environment of (a) Sn1, (b) Bi6 and (c) Bi7. The distances to the nearest Se atoms are shown.

structure of the mineral cannizzarite, $Pb_{46}Bi_{54}S_{127}$.[21] The layered structure of cannizzarite is composed of two different building units derived from the Bi_2Te_3 and the NaCl structure types. Bi_2S_3 layers have the Bi_2Te_3 structure type and alternate with PbS layers, which are two atoms thick. This motif is also found in the structure of $K_{0.66}Sn_{4.82}Bi_{11.18}Se_{22}$, which is highlighted in Fig. 2A. The layers in cannizzarite are flat and infinite. In contrast, the incorporation of potassium causes the break-up of the layers in $K_{0.66}Sn_{4.82}Bi_{11.18}Se_{22}$ so that only narrow sections of the cannizzarite structure are stabilized. The infinite PbS analogous layers are also broken down to three-metal octahedra wide ribbons that connect the step-shaped Bi_2Se_3 layers. The recognizable cannizzarite block in the structure is highlighted in Fig. 2A.

Properties

The electrical conductivity of an ingot of $K_{0.66}Sn_{4.82}Bi_{11.18}Se_{22}$ was measured to be 450 S cm^{-1} at room temperature. The thermopower of compacted samples of $K_{0.66}Sn_{4.82}Bi_{11.18}Se_{22}$ was measured in the temperature range 80–300 K and 300–600 K. However, for different extents of doping level from preparation to preparation (probably because of selenium vacancies) we observed values for the Seebeck coefficient at room temperature ranging from -20 to -50 μV K^{-1}. All samples measured possessed n-type behavior indicating that electrons are the dominant charge carriers. A typical value was a moderate -43 μV K^{-1} at room temperature. Fig. 4 displays the temperature dependence of the thermopower for the two measured temperature ranges. The thermopower increases steadily up from -13 μV K^{-1} at 80 K to -98 μV K^{-1} at 600 K.

The thermal conductivity of $K_{0.66}Sn_{4.82}Bi_{11.18}Se_{22}$ was measured for temperatures between 80 and 270 K. As shown in Fig. 5 the thermal conductivity is low and well in the range of suitable thermoelectric materials; it increases with rising temperature from 0.8 W m^{-1} K^{-1} (80 K) to 1.4 W m^{-1} K^{-1} (270 K). The thermal conductivity of the structurally related compound $K_{1+x}Pb_{4-2x}Bi_{7+x}Se_{15}$ covers the same range (0.8–1.4 W m^{-1} K^{-1}).[11] The low thermal conductivity of the

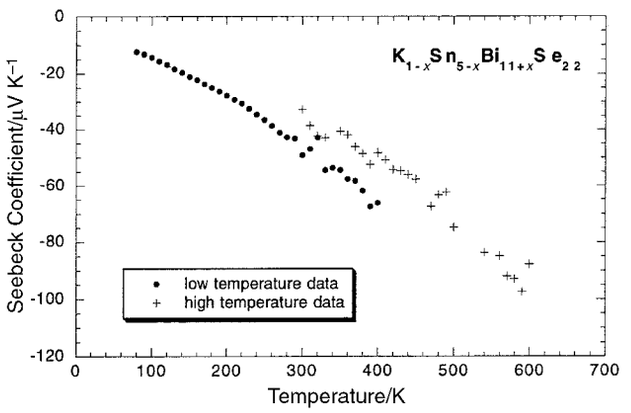

Fig. 4 Variable-temperature thermoelectric power data for a pressed pellet sample of $K_{0.66}Sn_{4.82}Bi_{11.18}Se_{22}$. Black dots indicate the low temperature data and the crosses show the high temperature measurements.

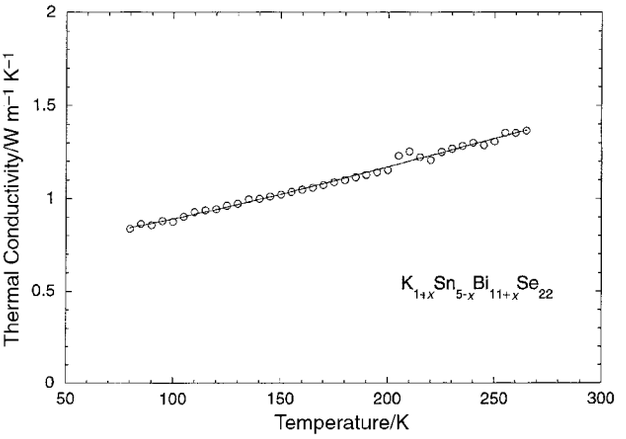

Fig. 5 Variable-temperature total thermal conductivity data of a polycrystalline ingot sample of $K_{0.66}Sn_{4.82}Bi_{11.18}Se_{22}$.

potassium tin bismuth selenide reported here is similar to the one of optimized $Bi_{2-x}Sb_xTe_3$ (1.5 W m^{-1} K^{-1}).[4] It is also comparable to that of the ternary potassium bismuth selenides β-$K_2Bi_8Se_{13}$ (0.8–1.6 W m^{-1} K^{-1})[8] and $K_{2.5}Bi_{8.5}Se_{14}$ (1.2–2.3 W m^{-1} K^{-1}).[8] The presence of extended disorder of the metal atoms and the probable "rattling" property of the potassium atoms are believed to be responsible for the very low thermal conductivity of $K_{0.66}Sn_{4.82}Bi_{11.18}Se_{22}$.

The optical absorption spectrum in the range of 0.1 to 0.5 eV at room temperature shows an extremely narrow energy band gap of ~0.12 eV. This small gap is responsible for the high room temperature conductivity of the material.

According to the DTA experiment and based on experiments done on bulk samples, $K_{0.66}Sn_{4.82}Bi_{11.18}Se_{22}$ melts congruently at 680 °C and recrystallizes at 663 °C.

Concluding remarks

Synthetic investigations of the system K/Sn/Bi/Se lead to the quaternary bismuth selenide narrow band gap semiconductor $K_{1-x}Sn_{5-x}Bi_{11+x}Se_{22}$, a material with a new structure type. Due to an extensive disorder of the metal atoms and the presence of "rattling" potassium atoms, $K_{1-x}Sn_{5-x}Bi_{11+x}Se_{22}$ has a low thermal conductivity. This makes it interesting for further investigations into its electrical and doping properties. The material has natural n-type doping and this may be amenable to manipulation with changes in the value of x.

Acknowledgements

We thank Dr. Ctirad Uher for his suggestions on the charge transport measurements. Financial support from the Office of Naval Research (Grant No. N00014-98-1-0443) and the Deutsche Forschungsgemeinschaft is gratefully acknowledged. This work made use of the SEM facilities of the Center for Electron Optics at Michigan State University.

References

1 (*a*) *Thermoelectric Materials 1998—The Next Generation Materials for Small-Scale Refrigeration and Power Applications*, ed. T. M. Tritt, M. G. Kanatzidis, G. D. Mahan and H. B. Lyon, *Mater. Res. Soc. Symp. Proc.*, 1998, p. 545; (*b*) *Thermoelectric Materials—New Directions and Approaches*, ed. T. M. Tritt, M. G. Kanatzidis, H. B. Lyon and G. D. Mahan, *Mater. Res. Soc. Symp. Proc.*, 1998, p. 478.

2 *CRC Handbook of Thermoelectrics*, ed. D. M. Rowe, CRC Press, Boca Raton, 1995.

3 (*a*) G. A. Slack, in *CRC Handbook of Thermoelectrics*, ed. D. M. Rowe, CRC Press, Boca Raton, 1995, p. 407; (*b*) G. A. Slack, in *Solid State Physics*, ed. H. Ehrenreich, F. Seitz and D. Turnbull, Academic, New York, 1997, vol. 34, p. 1; (*c*) B. C. Sales, *Mater.*

Res. Bull., 1998, **23**, 15; (*d*) B. C. Sales, D. Mandrus, B. C. Chakoumakos, V. Keppens and J. R. Thompson, *Phys. Rev. B*, 1997, **56**, 15081; (*e*) T. M. Tritt, *Science*, 1996, **272**, 1276; (*f*) M. G. Kanatzidis and F. J. DiSalvo, *ONR Quart. Rev.*, 1996, **XXVII**, 14.

4 (*a*) H.-H. Jeon, H.-P. Ha, D.-B. Hyun and J.-D. Shim, *J. Phys. Chem. Solids*, 1991, **4**, 579; (*b*) L. R. Testardi, J. N. Bierly Jr. and F. J. Donahoe, *J. Phys. Chem. Solids*, 1962, **23**, 1209; (*c*) C. H. Champness, P. T. Chiang and P. Parekh, *Can. J. Phys.*, 1965, **43**, 653; (*d*) C. H. Champness, P. T. Chiang and P. Parekh, *Can. J. Phys.*, 1967, **45**, 3611; (*e*) M. V. Vedernikov, V. A. Kutasov, L. N. Lukyanova and P. P. Konstantinov, *Proc. of the XVIth Int. Conf. On Thermoelectrics (ITC '97)*, Dresden, Germany, 1997, p. 56; (*f*) M. Stordeur, in *CRC Handbook of Thermoelectrics*, ed. D. M. Rowe, CRC Press, Boca Raton, 1995, p. 239.

5 (*a*) L. D. Hicks and M. S. Dresselhaus, *Phys. Rev. B*, 1993, **47**, 12727; (*b*) L. D. Hicks and M. S. Dresselhaus, *Phys. Rev. B*, 1993, **47**, 16631; (*c*) L. D. Hicks, T. C. Harmann and M. S. Dresselhaus, *Appl. Phys. Lett.*, 1993, **63**, 3230; (*d*) D. A. Broido and T. L. Reinecke, *Appl. Phys. Lett.*, 1995, **67**, 1170; (*e*) G. D. Mahan and H. B. Lyon, *J. Appl. Phys.*, 1994, **76**, 1899; (*f*) J. O. Sofo and G. D. Mahan, *Appl. Phys. Lett.*, 1994, **65**, 2690; (*g*) L. D. Hicks, T. C. Harmann, X. Sun and M. S. Dresselhaus, *Phys. Rev. B*, 1996, **53**, R10493.

6 D.-Y. Chung, S. Jobic, T. Hogan, C. R. Kannewurf, R. Brec and M. G. Kanatzidis, *J. Am. Chem. Soc.*, 1997, **119**, 2505.

7 (*a*) M. G. Kanatzidis, T. J. McCarthy, T. A. Tanzer, L.-H. Chen, L. Iordanidis, T. Hogan, C. R. Kannewurf, C. Uher and B. Chen, *Chem. Mater.*, 1996, **8**, 1465; (*b*) B. Chen, C. Uher, L. Iordanidis and M. G. Kanatzidis, *Chem. Mater.*, 1997, **9**, 1655.

8 M. G. Kanaktzidis, D.-Y. Chung, L. Iordanidis, K.-S. Choi, P. Brazis, M. Rocci, T. Hogan and C. Kannewurf, *Mater. Res. Soc. Symp. Proc.*, 1998, **545**, 233.

9 D.-Y. Chung, K.-S. Choi, L. Iordanidis, J. L. Schindler, P. W. Brazis, C. R. Kannewurf, B. Chen, S. Hu, C. Uher and M. G. Kanatzidis, *Chem. Mater.*, 1997, **9**, 3060.

10 D.-Y. Chung, T. Hogan, P. W. Brazis, C. R. Kannewurf and M. G. Kanatzidis, manuscript in preparation.

11 (*a*) D.-Y. Chung, K.-S. Choi, P. W. Brazis, C. R. Kannewurf and M. G. Kanatzidis, *Mater. Res. Soc. Symp. Proc.*, 1998, **545**, 65; (*b*) K.-S. Choi, D.-Y. Chung, A. Mrotzek, P. W. Brazis, C. R. Kannewurf and M. G. Kanatzidis, *Chem. Mater.*, submitted.

12 (*a*) W. W. Wendlandt and H. G. Hecht, *Reflectance Spectroscopy*, Interscience Publishers, New York, 1966; (*b*) G. Kotüm, *Reflectance Spectroscopy*, Springer-Verlag, New York, 1969; (*c*) S. P. Tandon and J. P. Gupta, *Phys. Status Solidi*, 1970, **38**, 363.

13 T. Hogan, N. Ghelani, S. Loo, S. Sportouch, S.-J. Kim, D.-Y. Chung and M. G. Kanatzidis, *Proceedings of the International Conference on Thermoelectrics*, 1999, p. 671.

14 O. Maldonado, *Cryogenics*, 1992, **32**, 908.

15 LabVIEW, Version 5.0, National Instruments, Austin, TX, 1999.

16 CERIUS^2, Version 1.6, Molecular Simulations, Inc., Cambridge, England, 1994.

17 SMART, Siemens Analytical X-ray Systems Inc., Madison WI, 1996.

18 SAINT V-4, Siemens Analytical X-ray Systems Inc., Madison, WI, USA, 1994–1996.

19 SADABS, Siemens Analytical X-ray Systems Inc., Madison WI, USA, 1994–1996.

20 SHELXTL V-5, G. M. Sheldrick, Siemens Analytical X-ray Systems Inc., Madison WI, USA, 1994.

21 E. Makovicky, in *Modern Perspectives in Inorganic Crystal Chemistry*, ed. E. Parthé, Kluwer Academic Publishers, The Netherlands, 1992, p. 131.